Comparison of three geostatistical methods for hydrofacies simulation: a test on alluvial sediments

Diana dell'Arciprete · Riccardo Bersezio · Fabrizio Felletti · Mauro Giudici · Alessandro Comunian · Philippe Renard

Abstract The hydrodispersive properties of porous sediments are strongly influenced by the heterogeneity at fine scales, which can be modeled by geostatistical simulations. In order to improve the assessment of the properties of three different geostatistical simulation methods (Sequential indicator simulation, SISIM; Transition probability geostatistical simulation, T-PROGS; Multiple point simulation, MPS) a comparison test at different scales was performed for a well-exposed aquifer analogue. In the analysed volume (approximately 30,000m^3) four operative hydrofacies have been recognised: very fine sand and silt, sand, gravelly sand and open framework gravel. Several equiprobable realizations were computed with SISIM, MPS and T-PROGS for a test volume of approximately 400m^3 and for the entire volume, and the different outcomes were compared with visual inspection and connectivity analysis of the very or poorly permeable structures. The comparison of the different simulations shows that the geological model is best reproduced when the simulations are realised separately for each highest rank depositional element and subsequently merged. Moreover, the three methods yield different images of the volume; in particular MPS is efficient in mapping the geometries of the most represented hydrofacies, whereas SISIM and T-PROGS can account for the distribution of the less represented facies.

Keywords Alluvial sediments · Aquifer characterization · Geostatistics · Hydrofacies · Heterogeneity

Received: 25 November 2010 / Accepted: 4 November 2011
Published online: 10 December 2011

Electronic supplementary material The online version of this article (doi:10.1007/s10040-011-0808-0) contains supplementary material, which is available to authorized users.

D. dell'Arciprete · M. Giudici (✉)
Dipartimento di Scienze della Terra "A. Desio",
Università degli Studi di Milano,
via Cicognara 7, 20129 Milano, Italy
e-mail: mauro.giudici@unimi.it

F. Felletti
Dipartimento di Scienze della Terra "A. Desio",
Università degli Studi di Milano,
via Mangiagalli 34, 20133 Milano, Italy

R. Bersezio
Dipartimento di Scienze della Terra "A. Desio",
Università degli Studi di Milano, CNR – IDPA,
via Mangiagalli 34, 20133 Milano, Italy

A. Comunian · P. Renard
Centre of Hydrogeology and Geothermics,
University of Neuchâtel,
Rue Emile Argand, 11, 2000 Neuchatel, Switzerland

Introduction

Progress towards improved characterization and modeling of porous groundwater reservoirs requires the integration of several different methods and involves the use of multiple data-sets, consisting of both descriptive "soft" geological data and "hard" sedimentological and hydrological parameters. Hard data are usually available in correspondence of wells and are often distributed in space by stratigraphic correlations and geostatistical interpolations. This paper focuses on the modeling of the hydrofacies distribution in a mixed-bedload/suspended-load alluvial aquifer analogue, using different geostatistical techniques calibrated on the direct observation of the lithofacies/hydrofacies distribution and sedimentary architecture on outcrops. Different geostatistical simulation methods are available to achieve such a goal (Deutsch 2002).

In this study, lithofacies distribution was simulated by three pixel-based simulation methods which are commonly used for water and oil reservoir modeling: sequential indicator simulation (SISIM; Goovaerts 1997; Deutsch and Journel 1998), transition probability geostatistical simulation (T-PROGS; Carle and Fogg 1996; Ritzi 2000; Lee et al. 2007) and multiple point simulation (MPS; Strebelle 2002; Liu et al. 2005). Pixel-based algorithms for facies modeling are fast and allow direct hard-data conditioning, avoiding iterative time-consuming approaches. These techniques permit simulation of the different facies in the form of coded indicator-type variables, where each value corresponds to a given facies.

Traditional geostatistical methods such as SISIM and T-PROGS, are based on random function models, chosen according to the geometrical affinity of their outcomes

 DOI 10.1007/s10040-011-0808-0

with the geological architecture under investigation. The model parameters (e.g., facies proportion, object density, variogram, etc.) are inferred from available quantitative data, and the model realizations are generated and conditioned to these data. This approach is effective in practice provided that the structure of the random function model captures the geometrical features. Although this approach has been successfully applied to many cases, it is not always possible to build a random function model which represents some complex geological architectures, for instance, in a meandering channel system. MPS was proposed by Guardiano and Srivastava (1993) for modeling subsurface heterogeneity. The first efficient implementation of the method was developed by Strebelle (2002) and it started to be an active research topic in recent years. Unlike traditional geostatistical simulations based on analytical random function models, MPS does not utilize such an explicit definition of a random function. It makes direct use of empirical multivariate distributions inferred from training images. MPS is applicable to any geological environment, provided that (1) a training image representative of the geological heterogeneity is available and (2) the essential features of this training image can be expressed by statistics defined on a configuration involving few points (Hu and Chugunova 2008). Some authors (Ortiz and Deutsch 2004; Ortiz and Emery 2005; Bastante et al. 2008) proposed to include multiple point statistics into sequential indicator approaches. In particular, Ortiz and Deutsch (2004) and Bastante et al. (2008) tested such an approach for applications to mining resource evaluation and showed how the introduction of multiple-point statistics could improve the results. Comparison of the applications of sequential indicator simulations and MPS approaches to map the secondary porosity of carbonate rocks, starting from computer tomography images, suggested that the geometry of the edges is more rounded and more similar to the actual images for MPS than for SISIM (Casar-González 2001). The comparison between truncated pluri-Gaussian simulations, sequential indicator simulations and multiple point simulations of a channel-fill turbidite sandstone analog (Falivene et al. 2006) in the Eocene Ainsa basin (northeast Spain) shows that variance based methods fail to capture the undulations of facies levels. On the other hand, multiple-point models do capture and reproduce more continuous and undulating hetherolithic and mud beds, but not as accurately as was done by object-based modeling methods, which provide the more realistic results for this test. Also Scheibe and Murray (1998) compare sequential Gaussian simulation with sequential indicator simulation and a Markov chain approach and conclude that it is important to recognize the differences between the simulation methods in order to choose the proper one taking into account both the geological structure to be modeled and the kind of predictions for which the model will be used.

Such comparisons have often considered the connectivity of the very or poorly permeable structures (Alabert et al. 1992; Zinn and Harvey 2003), an important feature when characterizing aquifers and reservoirs with respect to their flow properties. He et al. (2009) compare SISIM and T-PROGS to model clay content in soils and report better results for T-PROGS, as regards both the reproduction of minor classes and connectivity. An example of comparison of connectivity obtained with Gaussian and indicator-based non-Gaussian models is given by Journel and Alabert (1989). Failing to capture subsurface connectivity may bias the forecasts of any underground fluid flow and transport modeling project (Gómez-Hernández and Wen 1998; Knudby and Carrera 2005; Klise et al. 2009). This concept has been seldom treated systematically and only a few authors have used connectivity in order to compare results of different flow and transport models (Alabert et al. 1992; Zinn and Harvey 2003; Knudby and Carrera 2005); recently, some authors used the connectivity information to constrain the stochastic simulations (Renard and Caers 2008). An alternative approach to pixel-based methods is given by object-based methods, which are not considered in this paper: these two approaches have been compared with each other by, for example, Journel et al. (1998); Seifert and Jensen (2000), and Falivene et al. (2006).

The aim of this work is to compare the performances of SISIM, T-PROGS and MPS when applied to complex alluvial sediments, like point-bar/channel systems, and at different scales. The test was conducted on an aquifer analogue which was exposed in a sand-gravel quarry dug in the Lambro Valley (northern Italy, just south of the Milan conurbation). Here the analysis is focused on the characterization of hydrofacies heterogeneity. This is part of a research project described by dell'Arciprete (2010) and summarized by dell'Arciprete et al. (2010c), which includes also the assessment of the effects that fine-scale heterogeneity has on flow and transport properties by numerical experiments. A preliminary comparison between SISIM and T-PROGS for the whole volume is given by dell'Arciprete et al. (2010a), whereas a preliminary comparison among the three simulation methods can be found in dell'Arciprete et al. (2010c). Within this framework, the specific goal of this paper is to provide a quite broad and thorough description of the tests performed with the three simulation methods in order to improve the understanding of the strengths and the weaknesses of SISIM, T-PROGS and MPS at different scales and with a varying ratio between the numbers of the conditioning data and of the simulated grid cells.

In the next section the case study and the methods are briefly summarized. After this, a description of the data set used for the geostatistical simulations is provided, before the presentation of the principal results and the relative discussion.

Case study and methods

The geological environment of the study site is a Holocene point-bar–channel system of the Lambro River, a left tributary of the Po River that flows south of Milan (Italy) encased in a terraced valley. The sediments belong to an intermediate terrace located between the present-day river course and the last glacial maximum alluvial plain.

 DOI 10.1007/s10040-011-0808-0

The aquifer analogue was exposed in a sand-gravel open-air quarry, the so called "Ca' de Geri quarry site", located in Sant'Angelo Lodigiano, south of Milan (Fig. 1).

This area was chosen because a large exposure of sediments belonging to two different phases of the river's evolution could be studied. The sediments were progressively removed during quarrying, so it was possible to study the internal architecture of the point-bar and channel system, by the analysis of different outcrops. In the same area, before the removal of the sandy-gravel material, geophysical surveys were conducted in order to support the reconstruction of the external geometry of the sedimentary bodies (Mele 2004; Bersezio et al. 2007). The analyzed volume is approximately 30,000 m^3 (47 m×75 m×8.6 m), covering a horizontal surface of about 3,500 m^2.

The quarry site exposed three superimposed depositional units formed by sands, gravels and subordinate silt and clay, which could be attributed to an historical age, as it was proved by the findings of Roman to Middle Age and Renaissance Age artifacts (bricks, tiles, ceramics), imbricated within dunes and bars (dell'Arciprete 2005; Bersezio et al. 2007). Two units correspond to the exposed parts of two composite point bars and channels with minor channel fills on top. They were named respectively unit A (the lower, with Roman-Middle Age findings) and unit B (the upper, with Renaissance Age findings). Unit A shows the lateral transition from a composite point bar to main channel fill, and unit B is mostly represented by a composite point bar, with chute channel scour and fills on top. A younger channel (unit C, bounded by the erosion surface β and partly anthropogenic) eroded part of unit B. Together with units A and B, unit C is cut by the modern and present-day courses of the Lambro River.

The simulation methods require conditioning data, which, for this case study, are taken from the vertical facies maps of five almost orthogonal quarry faces. For modeling purposes a classification was adopted that is based on four hydrofacies that were defined after permeametric analyses on samples (dell'Arciprete et al. 2010a, 2010b): least permeable hydrofacies (F+fS refers to very fine sand (fS) and silt-clay (F) from topmost channel-fill, silt/clay plugs, drapes and balls), poorly permeable hydrofacies (S refers to sand from point-bar and channel fill bedforms), permeable hydrofacies (SG+GS is sandy gravel, SG, and gravelly sand, GS, from point bars) and most permeable hydrofacies (G is open framework gravels from the lower parts of the lateral accreted units). F+fS may be referred to as F for short, and SG+GS may be referred to as SG for short.

The geostatistical simulations were performed on three different domains (Fig. 2):

1. A *test volume* (11.4 m×11.4 m×2.85 m) discretized with small (0.2 m×0.2 m×0.05 m) cells or fine grid. This test volume was chosen in an area where many conditioning data, belonging to two orthogonal quarry faces, were available covering part of the three units A, B and C (Fig. 2);
2. The *entire volume* (46 m×74 m×8.4 m) discretized with large (0.4 m×0.4 m×0.1 m) cells or coarse grid;
3. The entire volume discretized with *fine grid* (0.2 m×0.2 m×0.05 m).

Notice that the Cartesian coordinates x, y and z correspond to west–east, south–north and bottom-up directions, respectively.

In order to evaluate efficiency and pitfalls of the different techniques, at different operative scales, the entire volume was reconstructed in two different ways: (1) simulating the undivided entire volume; (2) simulating separately the units, then merging the simulations through the α boundary that separates units A and B, which was obtained after kriging of the data points from logging and a ground penetrating radar survey.

The size of the cells was chosen in order to capture the heterogeneities at the hydrofacies scale. This size allows the simulations to be elaborated, allocating a reasonable computation time using a PC or a workstation. A short description of some properties of the simulation methods is given in the following.

Sequential indicator simulation (SISIM)

SISIM is based on the indicator variograms for the different facies and has been applied at different scales in a variety of depositional settings such as alluvial (Journel et al. 1998; Seifert and Jensen 1999; Zappa et al. 2006; Felletti et al. 2006; Falivene et al. 2007), deltaic (Cabello et al. 2007), aeolian (Sweet et al. 1996), and

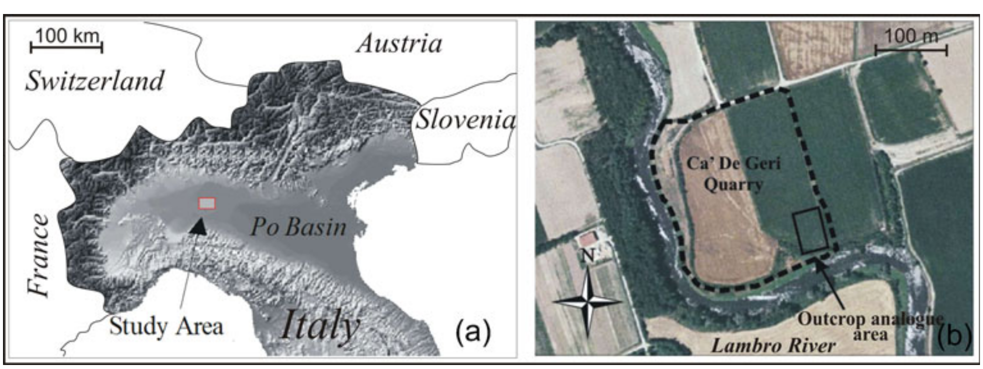

Fig. 1 Location map of **a** the study area in Italy and **b** the case study site

 DOI 10.1007/s10040-011-0808-0

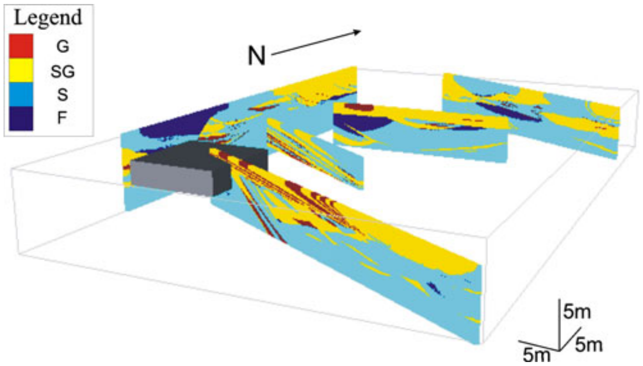

Fig. 2 Domain of the geostatistical simulation. Discretization of the facies maps after hydrofacies classification, and location of the test volume, are shown

deep-marine "turbiditic" settings (Journel and Gómez-Hernández 1993; Falivene et al. 2007).

There are legitimate criticisms against SISIM: (1) the models can appear very patchy and unstructured; (2) indicator variograms use two-point statistical measures only; (3) SISIM often leads to uncontrolled and geologically unrealistic transitions between the simulated categories; (4) the cross correlation between multiple categories is not explicitly controlled. Despite these criticisms, there are many good reasons to consider SISIM: (1) the required statistical parameters are easy to infer from limited data sets; (2) the simulation results are reasonable in settings where large-scale curvilinear features are absent; (3) the algorithm is robust and provides a straightforward way to transfer uncertainty in categories through the resulting numerical models. Semivariogram computation and SISIM were performed using GSLib (Deutsch and Journel 1998).

Transition probability geostatistical simulation (T-PROGS)

T-PROGS is based on the probabilities of transitions from one facies to another and on the modeling of such probabilities with Markov chains (Fogg et al. 1998; Carle et al. 1998). It has been applied to model facies distribution in braided rivers (Felletti et al. 2006), in alluvial fans (Fogg et al. 1998; Carle et al. 1998; Weissmann et al. 1999; Weissmann and Fogg 1999; Fleckenstein et al. 2006) and in glaciofluvial depositional systems (Proce et al. 2004). Other methods profit from the use of the Markov chain approach within the Bayesian-maximum entropy view (Christakos 1990; Bogaert 2002) as proposed, for example, by Allard et al. (2011) and by Zhang and Li (2007).

All the steps for simulations, including visualization, are implemented with the T-PROGS library of FORTRAN programs. Transition probability matrices are generated using GAMEAS (Carle 1999), a modification of the GSLIB (Deutsch and Journel 1998) code GAMV for estimating spatial statistics from irregularly spaced data. Transition probabilities in the horizontal plane are assumed isotropic; separate transition probabilities are determined for the vertical direction. Markov chain models are generated using MCMOD (Carle 1999). Finally, simulation is performed with TSIM (Carle 1999).

Multiple point simulation (MPS)

MPS has been proposed and developed quite recently (Caers 2001; Strebelle 2002; Liu et al. 2004; Straubhaar et al. 2011) and it has been used to reconstruct turbiditic reservoirs using three-dimensional (3D) training images and conditioning data from boreholes and geophysical prospecting (Strebelle et al. 2003); also 3D reconstructions starting from 2D training images at the pore scale have been proposed by Okabe and Blunt (2005).

At each grid node, the conditional probability density function (PDF) of the facies is obtained by considering hard data, previously simulated nodes and training images. The training image provides a conceptual description of the geological heterogeneity. It is analyzed within a template of fixed dimension; all the possible patterns embedded in that template are counted. This allows one to evaluate the conditional probability that a given facies is found at the node to be simulated from the conditioning data and the previously simulated nodes.

Multiple-point geostatistics should represent an improvement with respect to the classical variogram-based geostatistical methods because it characterizes the spatial structure by considering more than two data points (spatial configurations of several points are searched for in this method, whereas variograms account for correlation between pairs of points only), enabling the reproduction of complex patterns.

A difficulty of the MPS approach is in providing adequate training images that correspond to conceptual representations of the heterogeneity to be reproduced. The images depict the patterns of geological heterogeneities deemed relevant to the application under study. The training images do not carry any locally accurate information on the real structure; they merely reflect a prior geological/structural concept. Thus, a training image can be an unconditional realization generated by an object-based algorithm, or a simulated realization of an analogous field, or simply a geologist's sketch processed

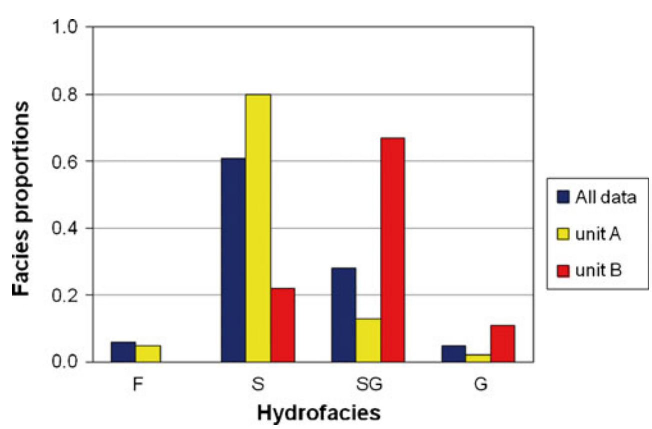

Fig. 3 Facies proportions computed in the conditioning faces for the whole volume and for units A and B separately

DOI 10.1007/s10040-011-0808-0

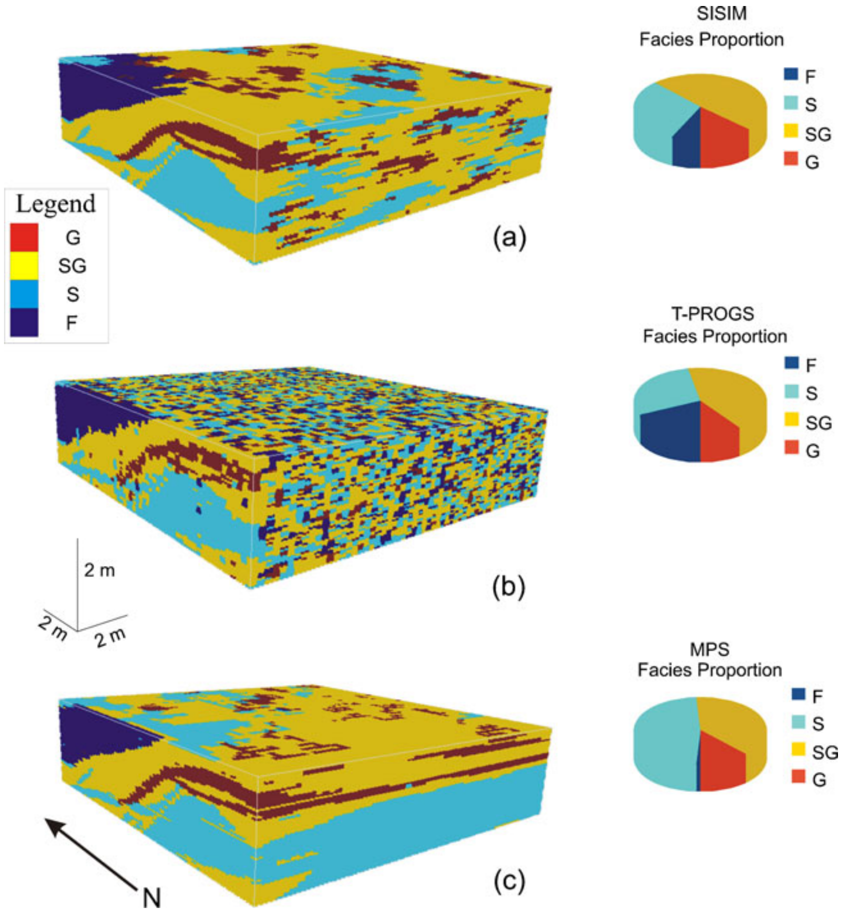

Fig. 4 Randomly selected simulations computed in the test volume with **a** SISIM **b** T-PROGS and **c** MPS. The facies proportions in the simulated volumes are shown in the pie charts

with computer-aided design tools and properly digitized (Strebelle 2002). In this study the discretized vertical facies maps were used as training images. This poses a problem because these images include non stationarity and are only two dimensional while MPS requires a 3D training image to generate a 3D simulation (see discussion in Comunian et al. 2010). Different techniques are currently under development to overcome that difficulty. Here, MPS was performed with a customized version of the code IMPALA (Straubhaar et al. 2011). More precisely, the simulations use two perpendicular training images. The conditional probability density distributions computed from these two images in two different directions are combined following the same principle as Okabe and Blunt (2005) but instead of using a linear combination of the individual PDFs, a multiplicative formula proposed by Bordley (1982) was used. In that formula, a weight of 0.5 was given to both PDFs extracted from the two perpendicular training images; moreover, facies proportions are not explicitly introduced in the simulation.

To compare the results obtained by the different geostatistical techniques, connectivity indicators have been used. Several definitions of connectivity can be given (Vassena et al. 2009). In this study, two indicators of facies connectivity are computed: total and intrinsic connectivity. They are based on the probability that pairs of connected points belong to a subset, characterized by a given property, e.g. texture or hydraulic conductivity, as proposed in Vassena et al. (2009). In particular the total connectivity of a facies is the probability that two, non coincident, points of the domain belonging to the given facies are connected; the intrinsic connectivity is the probability that two points are connected, conditioned on the fact that both belong to the given facies. Total connectivity depends not only on the intrinsic connectivity of the given facies, but also on the facies proportion, whereas intrinsic connectivity is largely independent of the facies proportion, as shown by simple examples in the appendix of Vassena et al. (2009). These indicators share some properties of the connectivity functions proposed by Allard et al. (1993); Allard (1994) and Western et al. (2001), but they do not depend upon the separation lag between the points.

Table 1 Input and output facies proportions in the *test volume*. The output proportions for the three simulation methods are expressed as mean±standard deviation over the ensemble of 50 realizations

	Input parameters	SISIM	T-PROGS	MPS
F	18 %	6.6%±1.3%	17.9%±0.2%	0.5%±0.2%
S	29 %	30.6%±3.7%	29.2%±0.2%	48.4%±4.8%
SG	43 %	49.4%±3.5%	42.9%±0.3%	39.5%±3.9%
G	10 %	13.4%±1.0%	10.0%±0.1%	11.6%±1.8%

DOI 10.1007/s10040-011-0808-0

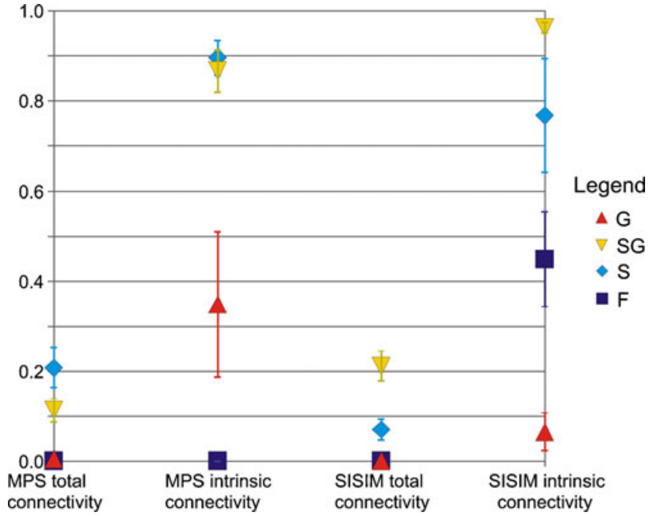

Fig. 5 Total and intrinsic connectivity (mean±standard deviation) computed on the test volume for the 50 simulations realized with SISIM and MPS

Dataset for the geostatistical simulation

The dataset used to compute the geostatistical simulations consists of:

1. *Facies proportions* computed on the vertical facies maps at different hierarchic levels (Fig. 3). In particular different facies proportions are used to simulate either units A and B separately or the whole volume. Note that the facies F is more abundant in the entire volume than in units A and B, because unit C is rich of fine sediments.
2. *Vertical facies maps* discretized with both small (0.2 m× 0.2 m×0.05 m) and large (0.4 m×0.4 m×0.1 m) cells.
3. Directional *variograms* for SISIM simulation, computed along the three space coordinates, for units A and B separately and for the whole volume, with both small and large cells. For the simulations of the test volume different variograms are computed, using data from the portions of the facies maps inside the test volume.
4. *Transition probabilities* for T-PROGS simulation, computed along the three space coordinates, for units A and B separately and for the whole volume, with both small and large cells.
5. The almost perpendicular facies maps were used as 2D training images for MPS simulations. The training images consist of two geological sections derived from the field observations. A template of 7×7 pixels was used in each direction, as well as four levels of multi-grid. The non stationarity displayed in the training images and in the simulation domain has not been treated explicitly.

Variogram models and transition probabilities are fitted to the experimental variograms and transitional probability curves, which were obtained separately for the three Cartesian coordinates. Some details (experimental and model variograms for SISIM, transition rate for T-PROGS, training images for MPS, etc.) are given in the electronic supplementary material (ESM).

Fifty simulations for each method (SISIM, T-PROGS and MPS) were performed on the test volume, which consists of 185,193 (57×57×57) cells; a portion of discretized facies maps inside the test volume (19,380 cells) was used as conditioning data. On the entire volume (coarse grid), 10 simulations were performed for each simulation method. For this volume, which consists of 1,787,100 (115×185×84) cells, all the discretized facies maps (i.e. 30,116 cells) were used as conditioning data. On the entire volume (fine grid) one simulation for each method was performed in order to limit computing times for facies modeling. In a first attempt, the undivided volume (236×373×172=15,140,816 cells) was simulated using all the discretized facies maps (120,868 cells) as conditioning data. A second simulation was obtained by simulating the separate units A and B (with respectively 78,435 and 28,372 cells as conditioning data), and then by cutting and merging the two simulated fields across the kriged α boundary between units A and B.

To achieve the goals of this work it is important to validate the results, i.e., to check whether the simulation

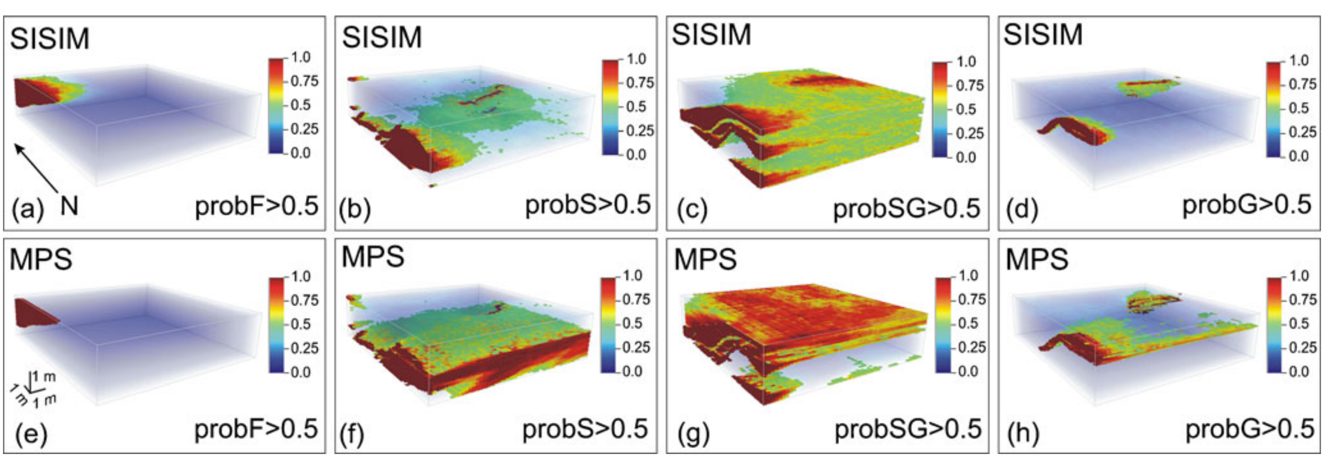

Fig. 6 Probability of finding each facies for the test volume with SISIM: **a** facies F, **b** facies S, **c** facies SG, **d** facies G, and with MPS, **e** facies F, **f** facies S, **g** facies SG, **h** facies G. The drawn regions correspond to the zones where the probability is greater than 0.5

 DOI 10.1007/s10040-011-0808-0

results reproduced the statistical parameters of the real distribution of the hydrofacies; however, even more important is the assessment of similarities and differences among the results of the three simulation methods. The comparisons between the geological model and the simulation results and among different simulation methods are performed in four different ways:

1. Visual inspection of the simulated volumes
2. 3D representation of the probability of occurrence of each facies
3. Comparative image analysis of the vertical facies maps and of sections cut through the simulated volumes at increasing separation from the conditioning data
4. Connectivity analysis

Discussion of the results

Test volume

For each simulation method, one realization is randomly selected out of the 50 simulations obtained for the test volume and is shown in Fig. 4. The mean and the standard deviation of facies proportions for the 50 simulations are reported in Table 1. The facies proportions in the simulated volumes are different from the proportions used as input parameter, because of the averaging effect between the conditions imposed by different parameters (conditioning data, proportions, variograms, etc). For SISIM, the final proportions are highly dependent on the relative positions of conditioning data and of the points randomly chosen to be simulated first. If these points are located next to the experimental data of a specific category, the proportion of simulated values of that category tends to increase rapidly, finally exceeding the global proportion, and it very rarely returns to the objective. This effect becomes more significant as the ranges of the indicator variograms increase and it mostly affects the categories with low global proportions (Soares 1998). In the case of MPS the training images represent the strongest constrain.

Total and intrinsic connectivity indicators computed in the *test volume* are displayed in the graph of Fig. 5. From the computation of the connectivity indicators, it can be observed that: (1) for MPS the total connectivity for facies S is higher than for facies SG, instead for SISIM the total connectivity for S facies is lower than for SG facies; (2) for MPS the intrinsic connectivity of S facies is close to the intrinsic connectivity of SG facies; (3) the intrinsic connectivity for G facies is less than 0.1 for SISIM simulations.

From the 50 equiprobable simulations of the test volume, the probability of occurrence for each facies was computed (Fig. 6). At this scale the following results can be highlighted.

1. It was almost impossible to find a Markov chain model fitting the transition probability statistics computed on

Table 2 Input and output facies proportions in the entire volume, coarse grid. The output proportions for the three simulation methods are expressed as mean±standard deviation over the ensemble of 10 realizations

	Input parameters	SISIM	T-PROGS	MPS
F	6%	6.8%±1.2%	6.8%±1.0%	2.6%±0.2%
S	61%	52.7%±3.1%	59.8%±1.1%	67.4%±1.4%
SG	28%	32.9%±2.5%	28.1%±1.0%	27.7%±1.4%
G	5%	7.6%±1.1%	5.3%±0.3%	2.3%±0.2%

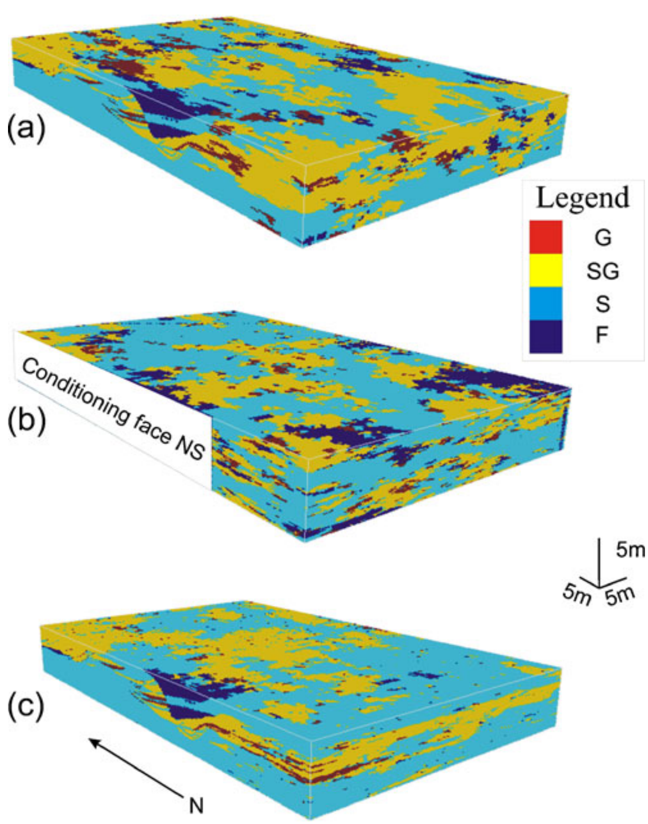

Fig. 7 Equiprobable simulation number 1 of 10, computed in the entire volume (0.4 m×0.4 m×0.1 m cells) with **a** SISIM **b** T-PROGS and **c** MPS

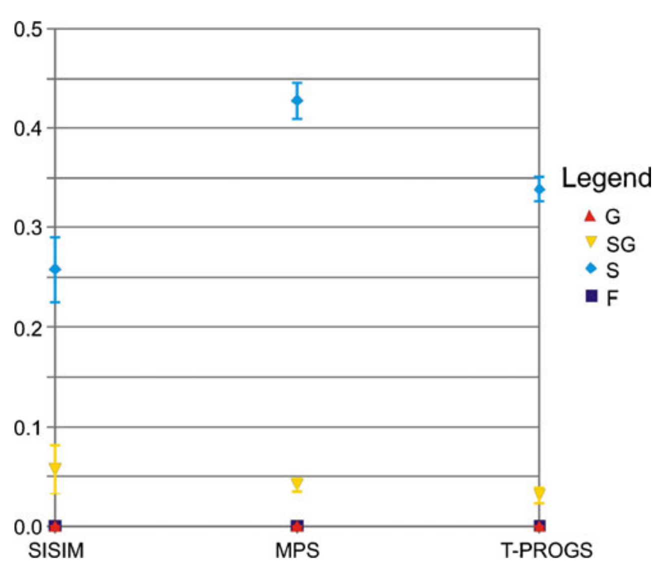

Fig 8 Total connectivity computed in the entire volume simulated with SISIM, MPS and T-PROGS with coarse grid

 DOI 10.1007/s10040-011-0808-0

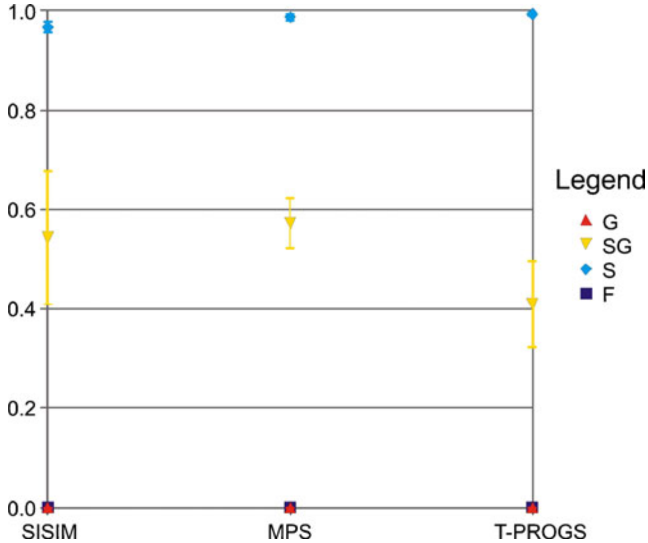

Fig. 9 Intrinsic connectivity computed in the entire volume simulated with SISIM, MPS and T-PROGS with coarse grid

the conditioning faces of the test volume. At this scale, in fact, there are few repetitions of the hydrofacies bodies (that mimic the sedimentary architectural elements), so that transition probability statistics are inadequate and therefore T-PROGS simulations are unsatisfactory for all facies at this scale (Fig. 4).

2. MPS reproduces laterally persistent hydrofacies bodies for the S, SG and G facies, which are the most abundant in the conditioning faces used to derive the training images. As a consequence, the MPS technique reproduces well connected volumes of the high permeability hydrofacies (SG and G), which could represent the preferential flow paths in the considered region of the aquifer analogue (Fig. 5). On the other hand, the same simulations cannot take into account the geometry and distribution of the F hydrofacies bodies. In order to improve the assessment of this minor facies, some tests were performed by changing the weights assigned to the PDFs of the two faces. However, since the F facies is present only in one of the orthogonal training images, it was necessary to assign a very small weight to the PDF of the other image in the probability aggregation formula; but in that case the F facies proportion was largely overestimated.
3. SISIM reproduces S, SG and G hydrofacies bodies that are less persistent than those generated by MPS; on the other hand all the simulated hydrofacies have a good and realistic spatial continuity (Fig. 6).

Entire volume, coarse grid

Figure 7 shows randomly selected examples of the realizations obtained on the *entire volume*, with the *coarse grid*, for each simulation method. The mean and the standard deviations of facies proportions for the 10 simulations are reported in Table 2. Notice that the proportions of F and G facies for the simulations with MPS are significantly lower than the input data, because this method reproduces the less abundant facies only partially.

Total and intrinsic connectivity indicators are displayed in the graphs of Figs. 8 and 9. From the 10 equiprobable simulations of the entire volume simulated with the coarse grid, the probability of occurrence for each facies was computed (Fig. 10). At this scale the following results can be highlighted.

1. T-PROGS simulations generate a background of S hydrofacies voxels, whereas the other hydrofacies are sparse through the whole volume. In contrast, MPS

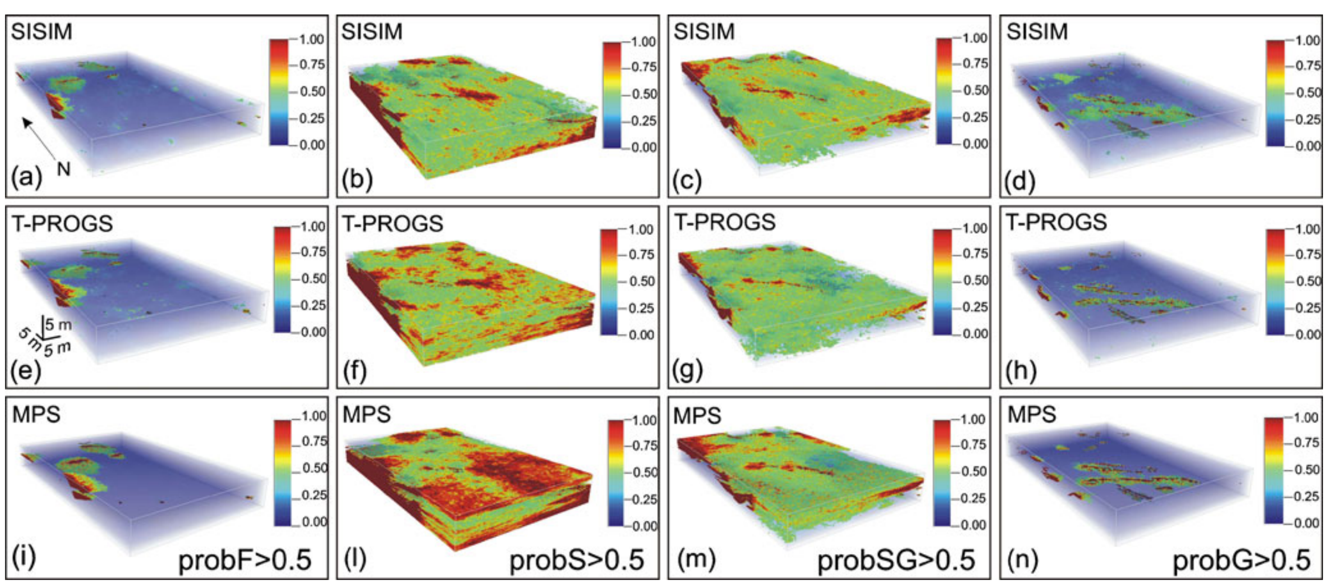

Fig. 10 Probability of finding each facies for the entire volume (coarse grid) with SISIM **a** facies F, **b** facies S, **c** facies SG, **d** facies G, with T-PROGS, **e** facies F, **f** facies S, **g** facies SG, **h** facies G, and with MPS, **i** facies F, **l** facies S, **m** facies SG, **n** facies G. The drawn regions correspond to the zones where the probability is greater than 0.5

DOI 10.1007/s10040-011-0808-0

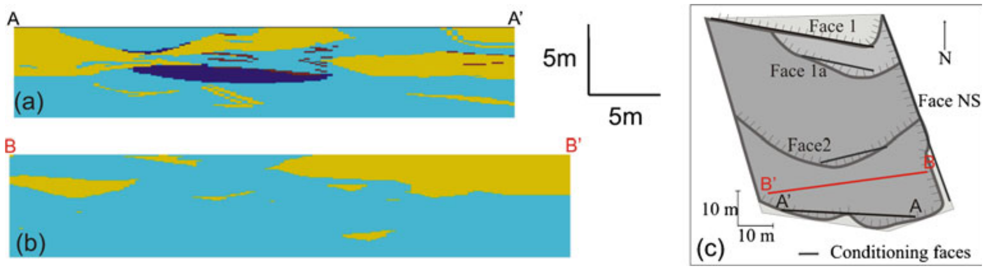

Fig. 11 **a** Training image face 3, discretized with coarse grid; **b** section cut into the MPS simulated volume (coarse grid, realization 4); **c** location of face 3 (A–A') and section B–B' (shown in **b**). From these pictures the similarity between the shape of the S and SG hydrofacies bodies in the simulated volume and in the training image are evident

simulations yield well connected volumes of SG hydrofacies bodies that alternate with the S hydrofacies bodies, in agreement with the conditioning data-set (Fig. 11).

2. MPS simulations can take into account the least represented hydrofacies (F and G, Fig. 7) only partially; nonetheless they can reproduce realistic shape and size of the most abundant S and SG hydrofacies. The most represented hydrofacies are reproduced by MPS simulations in the whole volume as bodies whose shape and size are very similar to those appearing in the training images (Fig. 11).
3. T-PROGS simulations yield a more connected pattern of the poorly permeable F hydrofacies, than the very permeable G hydrofacies. Both S and G hydrofacies are loosely connected in SISIM realizations (Figs. 8 and 9).

Entire volume, fine grid

Two simulations of the entire volume with the *fine grid* were obtained with each method, simulating either the whole undivided volume or the units A and B separately (unit C was not considered here, because of the very poor available observation). The results are shown in Fig. 12. In Table 3 facies proportions derived from the simulations are reported.

Total and intrinsic connectivity indicators were computed in the entire volume with the fine grid, for moving blocks (57×57×57 cells, corresponding to 11.4 m× 11.4 m×2.85 m); the results are displayed in Fig. 13. On the entire volume simulated with the fine grid, the following results can be highlighted.

1. Visual inspection and comparison with the facies maps and field observations show that SISIM and T-PROGS yielded unrealistic results for the undivided volume of units A and B. The realizations obtained with the separate simulation of the two units were by far more realistic (Fig. 12). In contrast, MPS yields more realistic simulations for the undivided volume than for the merge of the separate simulations of A and B. MPS takes into account the differences between the two units that are evident in the training images of the entire volume, and works better over large volumes than on small ones.
2. Image analysis shows that all the techniques underestimate spatial continuity and size of the low-rank geological elements (bodies composed of one hydrofacies) in the case of the simulations realized separately for A and B.
3. The connectivity analysis performed on the volume simulated with SISIM for units A and B separately was considered. In this case, the S hydrofacies is more abundant in unit A than in unit B. Nonetheless it looks to be well connected among the whole volume (high total connectivity in unit A, high intrinsic connectivity in both units A and B). In contrast, the SG hydrofacies

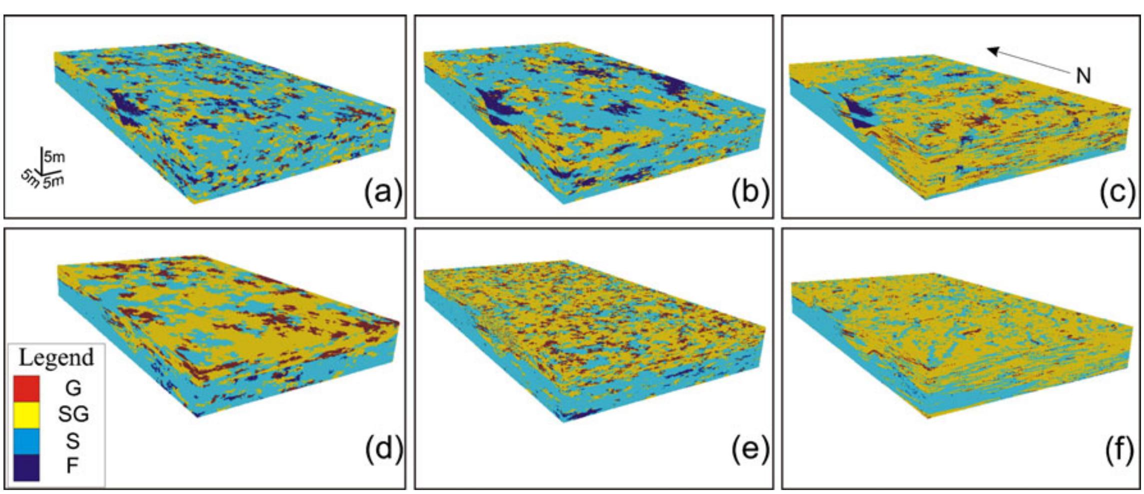

Fig. 12 Simulations of the undivided entire volume (0.2 m×0.2 m×0.05 m cells) computed with **a** SISIM, **b** T-PROGS and **c** MPS. Simulations of units A and B computed separately using **d** SISIM, **e** T-PROGS and **f** MPS

DOI 10.1007/s10040-011-0808-0

Table 3 Facies proportions of the entire volume, fine grid, simulated by SISIM, T-PROGS and MPS, for undivided volume and unit A+unit B

Undivided volume	Input parameters		SISIM	T-PROGS	MPS
F	6%		7.1%	6.8%	2.8%
S	61%		58.7%	59.3%	49.5%
SG	28%		28.8%	28.8%	43.5%
G	5%		5.4%	5.1%	4.2%
Unit A+unit B					
	unit A	unit B			
F	5.0%	0.0%	3.5%	3.8%	3.1%
S	80.0%	22.0%	56.8%	57.4%	50.1%
SG	13.0%	67.0%	33.1%	32.8%	44.8%
G	2.0%	11.0%	6.6%	6.0%	2.0%

is more abundant in unit B than in unit A where it shows a low connection degree. In the entire volume case, some areas of well connected F and G hydrofacies have been observed. However, the total connectivity is low (Fig. 13).

4. The distribution of hydrofacies G (open framework gravels along the lower part of the inclined bed-sets of the composite bars) and F (meter-sized lenses of very fine sand and mud at the top of minor channel elements and decimeter-size mud clasts at their base) is not reproduced by T-PROGS simulations, which yield a scattered pattern of small clusters, sparse in a background occupied by facies S and SG. MPS yields better results for background hydrofacies than for the least abundant ones (Fig. 12). Simulations by SISIM reproduced rather efficiently the size, shape, distribution and orientation (sloping features of lateral and frontal accreted elements) of these low-hierarchy elements (dell'Arciprete et al. 2010b, dell'Arciprete 2010).
5. The geological model shows non-stationary transition from SG and G hydrofacies association to S hydrofacies, and less abundant F hydrofacies moving towards the western and southern part of the volume, where the composite point-bar to channel-fill transitions occur. This trend is only partially reproduced by simulations. Visual inspection of the simulated volumes reveals periodical repetitions of the most permeable hydrofacies G, at a separation distance that is a multiple of the variogram range for SISIM and of the minimum of transition probability for T-PROGS. MPS yields a sort of repetition of S and SG bodies, imitating their shape in the training images. In summary, the simulation approaches used in this work do not account for the non-stationary architecture of composite bars and channels, and therefore do not properly reproduce the real spatial trends of these sedimentary structures and the number of connections.
6. SISIM and T-PROGS do not reproduce the low-rank components of the architectural complexity, like minor channels, erosion bases, etc. This problem affects many pixel-oriented methods of simulation and, in this case, it seems to arise from the fact that the semivariogram and correlation matrix are a bivariate measure (two-point autocorrelation), and therefore any non-linear correlation structure (e.g., curved surfaces) cannot be reproduced. MPS, in contrast, can reproduce the shape of the curved structures, but fails to reproduce their internal features at this scale. Moreover, vertical tendencies at the scale of the bed-sets and bed-set groups (in the range from 2 to 4 m), which are evident in the cross-variogram and in the off-diagonal vertical transition-probability plots of the facies maps, are partially lost in the 3D simulation. The representation of such non-stationary periodicities is still an open issue and cannot be resolved using "classical stationary" semivariogram or Markov chain models (Felletti et al. 2006).

A critical parameter in conditional simulations is the ratio between the number of conditioning data and the number of simulated cells. For the test volume this ratio is equal to 0.105; in this case, MPS and SISIM produce satisfactory simulations, whereas the differences between the simulations performed over the entire volume with the coarse grid (ratio equal to 0.017) and the fine grid (ratio equal to 0.008) show that the use of small cells does not significantly improve the results. In contrast, with MPS the shape and the size of S and SG hydrofacies bodies are partly lost. Differently, T-PROGS needs a significant number of object repetitions and gives unsatisfactory results for the test volume and for the unit B when simulated as a stand-alone body.

Simulations of the undivided volume are less realistic than simulations obtained separately for units A and B,

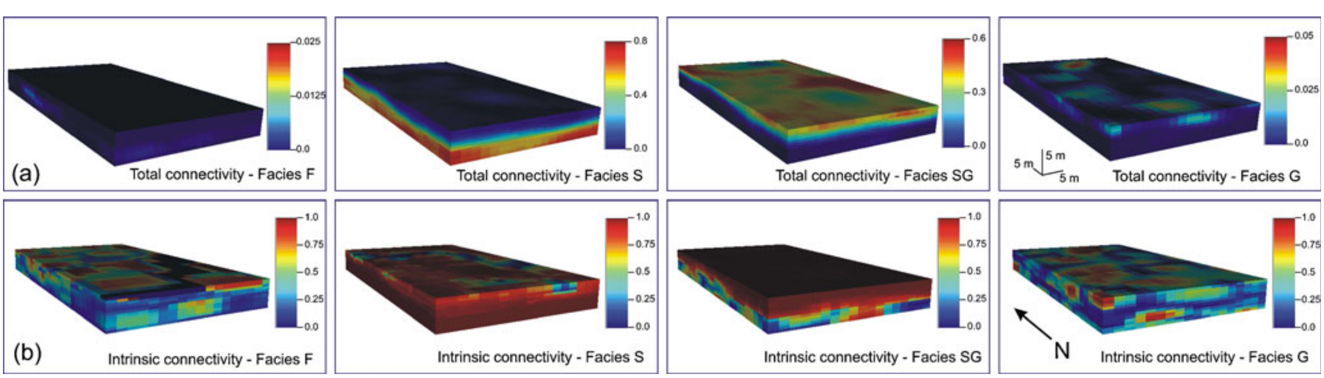

Fig. 13 **a** Total and **b** intrinsic connectivity computed in the SISIM simulated volume for moving blocks of 57×57×57 cells

 DOI 10.1007/s10040-011-0808-0

because these units are characterized by very different statistical properties (frequency and correlation of hydrofacies). In order to obtain realistic simulations it is necessary that statistical properties do not vary significantly throughout the studied domain (Falivene et al. 2007).

Conclusions

Three different pixel-oriented methods were applied to simulate hydrofacies distribution in a point-bar–channel aquifer analogue: SISIM, based on the facies correlation length derived from the variograms; T-PROGS, based on the transition probabilities, which take into account the juxtaposition of the different facies; MPS, based on the training images. Note that the MPS approach used here is not conventional since it is based on the use of 2D training images and a recombination of partial probability density functions, while the traditional approach uses a full 3D training image. Consequently the conclusions drawn on the MPS method may not be general. Still, this work emphasizes the difficulties related to the selection of a training image when using MPS in real field applications. From their distinctive characteristics the methods were expected to properly reproduce different features of the sedimentary heterogeneity: the length of the hydrofacies bodies for SISIM, the transition between hydrofacies (a proxy of their connectivity) for T-PROGS and the shape of the hydrofacies bodies for MPS.

The results of the distinct simulations show the different features of the analyzed volume effectively reproduced by each method. MPS can take into account the shape and size of the most abundant hydrofacies bodies, which must occur at least in two orthogonal training images, whereas SISIM and T-PROGS can reproduce efficiently the distribution of the less abundant facies.

To obtain realistic realizations with T-PROGS some repetitions of the analyzed hydrofacies bodies along the directions of the Cartesian axes are necessary. Otherwise transition probability statistics cannot be estimated with a sufficient accuracy, as it occurred in the simulations of the test volume.

The simulation methods, specifically SISIM and T-PROGS, yield more realistic results if units A and B are modeled separately, because stochastic simulations work better if the statistical properties of the simulated bodies are homogeneous (Falivene et al. 2007).

The geological model shows a well-defined trend along the NE direction, with a transition from prevailing gravels to fine-grained sediments (fine sands). The simulation methods used in this study take into account this non-stationary behavior only indirectly, since it is introduced through the data of the conditioning faces. The methods reproduce stationary volumes in such a way that the characteristics of the random repetitions of the hydrofacies bodies depend on the simulation method and on the parameters that characterize the underlying geostatistical model. In fact, the separation between hydrofacies bodies varies over multiples of the variogram ranges (for SISIM) or of the minimum transition probability (for T-PROGS). In the MPS simulations, the shapes of these bodies are similar to those appearing in the training images. The increasing abundance of the gravelly hydrofacies G in the upper part of the volume is better reproduced by MPS simulations, whereas it can be reproduced by SISIM and T-PROGS only if units A and B are simulated separately.

For an efficient pixel-oriented conditional simulation, a significant number of conditioning data is needed. The simulations of the entire volume with coarse grid, for example, are more realistic than the simulations of the entire volume with fine grid, even if the database has a better accuracy than the discretization grids. This fact is an effect of the ratio between the number of the conditioning data and the number of simulated cells, which is much greater for the coarse grid than for the small grid (1.7% vs. 0.8%). With the coarse grid simulations, however, the features of the low hierarchic level are lost.

Acknowledgements This work was financially supported by the Ministero dell'Istruzione, dell'Università e della Ricerca (MIUR) and the University of Milan through the research project of national interest "Integrated geophysical, geological, petrographical and modeling study of alluvial aquifer complexes characteristic of the Po plain subsurface: relationships between scale of hydrostratigraphic reconstruction and flow models" (PRIN 2007).

References

Alabert FG, Aquitaine E, Modot V (1992) Stochastic models of reservoir heterogeneity: impact on connectivity and average permeabilities. Society of Petroleum Engineers, Richardson, TX

Allard D (1994) Simulating a geological lithofacies with respect to connectivity information using the truncated Gaussian model. In: Armstrong M, Dowd PA (eds) Geostatistical Simulations 197–211. Kluwer, Dordrecht, The Netherlands

Allard D, The HERESIM Group (1993) On the connectivity of two random set models: the truncated Gaussian and the Boolean. In: Soares A (ed) Geostatistics Tróia, 92nd edn. Kluwer , Dordrecht, The Netherlands, pp 467–478

Allard D, D'Or D, Froidevaux R (2011) An efficient maximum entropy approach for categorical variable prediction. Eur J Soil Sci 62:381–393. doi:10.1111/j.1365-2389.2011.01362.x

Bastante FG, Ordóñez C, Taboada J, Matías JM (2008) Comparison of indicator kriging, conditional indicator simulation and multiple-point statistics used to model slate deposits. Eng Geol 98:50–59

Bersezio R, Giudici M, Mele M (2007) Combining sedimentological and geophysical data for high-resolution 3-D mapping of fluvial architectural elements in the Quaternary Po plain (Italy). Sediment Geol 202:230–248

Bogaert P (2002) Spatial prediction of categorical variables: the Bayesian maximum entropy approach. Stoch Env Res Risk A 16:425–448

Bordley R (1982) A multiplicative formula for aggregating probability assessments. Manage Sci 28:1137–1148

Cabello P, Cuevas JL, Ramos E (2007) 3D modelling of grain size distribution in Quaternary deltaic deposits (Llobregat Delta, NE Spain). Geol Acta 5:231–244

Caers J (2001) Geostatistical reservoir modelling using statistical pattern recognition. J Pet Sci Eng 29:177–188

Carle SF (1999) T-PROGS: transition probability geostatistical software version 2.1. University of California, Davis, CA

Carle SF, Fogg GE (1996) Transition probability-based indicator geostatistics. Math Geol 28:453–477

 DOI 10.1007/s10040-011-0808-0

Carle SF, Labolle EM, Weissmann GS, Van Brocklin D, Fogg GE (1998) Conditional simulation of hydrofacies architecture: a transition probability/Markov approach. In: Fraser GS, Davis JM (eds) Hydrogeologic models of sedimentary aquifers. Special Publication, Concepts in Hydrogeology and Environmental Geology, SEPM, Tulsa, OK, pp 147–170

Casar-González R (2001) Two procedures for stochastic simulation of vuggy formations. SPE Paper 69663, SPE, Richardson, TX

Christakos G (1990) A Bayesian/maximum entropy view to spatial estimation problem. Math Geol 30:435–462

Comunian A, Renard P, Straubhaar J, Bayer P (2010) Three-dimensional high resolution fluvio-glacial aquifer analog: part 2, geostatistical modeling. J Hydrol 40:10–23

dell'Arciprete D (2005) Caratterizzazione di un analogo di acquifero fluviale meandriforme [Characterisation of an aquifer analog in a meandering river environment], Degree Thesis, Università degli Studi di Milano, Italy

dell'Arciprete D (2010) Connectivity, flow and transport models in a point bar-channel aquifer analogue. PhD thesis, Università degli Studi di Milano, Italy

dell'Arciprete D, Felletti F, Bersezio R (2010a) Simulation of fine-scale heterogeneity of meandering river aquifer analogues: comparing different approaches. In: Atkinson PM, Lloyd CD (eds) geoENV VII – Geostatistics for Environmental Applications: quantitative geology and geostatistics 16: 127–137. Springer, Heidelberg, Germany

dell'Arciprete D, Bersezio R, Felletti F, Giudici M, Vassena C (2010b) Simulation of heterogeneity in a point-bar/channel aquifer analogue. Mem Descr Carta Geol Ital 90:85–96

dell'Arciprete D, Baratelli F, Bersezio R, Felletti F, Giudici M, Vassena C, Carrera J (2010c) Relating facies connectivity to flow and transport properties for a point bar-channel aquifer analogue. In: XVIII International Conference on Water Resources. CIMNE, Barcelona, 2010

Deutsch CV (2002) Geostatistical reservoir modeling. Oxford University Press, New York

Deutsch CV, Journel AG (1998) GSLIB: Geostatistical Software Library—and user's guide, 2nd edn. Oxford University Press, New York

Falivene O, Arbués P, Gardiner A, Pickup G, Muñoz JA, Cabrera L (2006) Best practice stochastic facies modeling from a channel-fill turbidite sandstone analog (the Quarry outcrop, Eocene Ainsa basin, northeast Spain). AAPG Bull 90:1003–1029

Falivene O, Cabrera L, Muñoz JA, Arbués P, Fernández O, Sáez A (2007) Statistical grid-based facies reconstruction and modelling for sedimentary bodies Alluvial-palustrine and turbiditic examples. Geol Acta 5:199–230

Felletti F, Bersezio R, Giudici M (2006) Geostatistical simulation and numerical upscaling, to model groundwater flow in a sandy gravel, braided river, aquifer analogue. J Sediment Res 76:215–1229

Fleckenstein JH, Niswonger RG, Fogg GE (2006) River-aquifer interactions, geologic heterogeneity, and low-flow management. Ground Water 44:837–852

Fogg GE, Noyes CD, Carle SF (1998) Geologically-based model of heterogeneous hydraulic conductivity in an alluvial setting. Hydrogeol J 6:131–143

Gómez-Hernández JJ, Wen XH (1998) To be or not to be multi-Gaussian? A reflection on stochastic hydrogeology. Adv Water Resour 21:47–61

Goovaerts P (1997) Geostatistics for natural resources evaluation. Oxford University Press, Oxford

Guardiano F, Srivastava RM (1993) Multivariate geostatistics: beyond bivariate moments. In: Soares A (ed) Geostatistics-Troia. Kluwer, Dordrecht, The Netherlands, pp 133–144

He Y, Hu K, Li B, Chen D, Suter HC, Huang Y (2009) Comparison of sequential indicator simulation and transition probability indicator simulation used to model clay content in microscale surface soil. Soil Sci 174:395–402

Hu LY, Chugunova T (2008) Multiple-point geostatistics for modeling subsurface heterogeneity: a comprehensive review. Water Resour Res 44:W11413

Journel AG, Alabert F (1989) Non-Gaussian data expansion in the earth sciences. Terra Nova 1:123–134

Journel AG, Gómez-Hernández JJ (1993) Stochastic imaging of the Wilmington Clastic Sequence. Society of Petroleum Engineers Formation Evaluation March, SPE, Richardson, TX, pp 33–40

Journel AG, Gundeso R, Gringarten E, Yao T (1998) Stochastic modelling of a fluvial reservoir: a comparative review of algorithms. J Pet Sci Eng 21:95–121

Klise KA, Weissmann GS, McKenna SA, Nichols EM, Frechette JD, Wawrzyniec TF, Tidwell VC (2009) Exploring solute transport and streamline connectivity using LiDAR-based outcrop images and geostatistical representations of heterogeneity. Water Resour Res. doi:10.1029/2008WR007500

Knudby C, Carrera J (2005) On the relationship between indicators of geostatistical, flow and transport connectivity. Adv Water Resour 28:405–421

Lee S-Y, Carle SF, Fogg GE (2007) Geologic heterogeneity and a comparison of two geostatistical models: sequential Gaussian and transition probability-based geostatistical simulation. Adv Water Resour 30:1914–1932

Liu Y, Harding A, Abriel W, Strebelle S (2004) Multiplepoint simulation integrating wells, 3D seismic data and geology. Am Assoc Pet Geol Bull 88:905–922

Liu Y, Harding A, Gilbert R, Journel A (2005) A workflow for multiple-point geostatistical simulation. In: Leuangthong O, Deutsch CV (eds) Geostatistics Banff 2004. Springer, Heidelberg, pp 245–254

Mele M (2004) Metodi geofisici e geologici per la caratterizzazione degli acquiferi [Geophysical and geological methods for aquifer characterisation]. Degree Thesis, Università degli Studi di Milano, Italy

Okabe H, Blunt MJ (2005) Pore space reconstruction using multiple-point statistics. J Pet Sci Eng 46:121–137

Ortiz JM, Deutsch CV (2004) Indicator simulation accounting for multiple-point statistics. Math Geol 36:545–565

Ortiz JM, Emery X (2005) Integrating multiple-point statistics into sequential simulation algorithms. In: Leuangthong O, Deutsch CV (eds) Geostatistics Banff 2004. Springer, Heidelberg, pp 969–978

Proce CJ, Ritzi RW, Dominic DF, Dai Zh (2004) Modeling multiscale heterogeneity and aquifer interconnectivity. Ground Water 42:658–670

Renard Ph, Caers J (2008) Conditioning facies simulations with connectivity data. In: Proceedings of the VIII Geostatistical Congress. Santiago, Chili, December 2008

Ritzi RW (2000) Behaviour of indicator variogram and transition probabilities in relation to the variance in lengths of hydrofacies. Water Resour Res 36:3375–3381

Scheibe TD, Murray CJ (1998) Simulation of geologic patterns: a comparison of stochastic simulation techniques for groundwater transport modelling In: Fraser GS, Davis JM (eds) Special publication of the SEPM (Society for Sedimentary Geology), Tulsa, OK, pp 107–118

Seifert D, Jensen JL (1999) Using sequential indicator simulation as a tool in reservoir description: issues and uncertainties. Geology 31:527–550

Seifert D, Jensen JL (2000) Object and pixel-based reservoir modeling of a braided fluvial reservoir. Math Geol 32:581–603

Soares A (1998) Sequential indicator simulation with correction for local probabilities. Math Geol 30:761–765

Straubhaar J, Renard P, Mariethoz G, Froidevaux R, Besson O (2011) An improved parallel multiple-point algorithm. Math Geosci 43:305–328. doi:10.1007/s11004-011-9328-7

Strebelle S (2002) Conditional simulation of complex geological structures using multiple-point statistics. Math Geol 34:1–21

Strebelle S, Payrazyan K, Caers J (2003) Modeling of a deepwater turbidite reservoir conditional to seismic data using principal component analysis and multiple-point geostatistics. SPE J 8:227–235

 DOI 10.1007/s10040-011-0808-0

Sweet ML, Blewden CJ, Carter AM, Mills CA (1996) Modeling heterogeneity in a low-permeability gas reservoir using geostatistical techniques, Hyde Field, southern North Sea. AAPG Bull 80:1719–1735

Vassena C, Cattaneo L, Giudici M (2009) Assessment of the role of facies heterogeneity at the fine scale by numerical transport experiments and connectivity indicators. Hydrogeol J. doi:10.1007/s10040-009-0523-2

Weissmann GS, Fogg GE (1999) Multi-scale alluvial fan heterogeneity modeled with transition probability geostatistics in a sequence stratigraphic framework. J Hydrol 226:48–65

Weissmann GS, Carle SF, Fogg GE (1999) Three-dimensional hydrofacies modeling based on soil surveys and transition probability geostatistics. Water Resour Res 35:1761–1770

Western A, Bloschl G, Grayson RB (2001) Toward capturing hydrologically significant connectivity in spatial patterns. Water Resour Res 37:83–97

Zappa G, Bersezio R, Felletti F, Giudici M (2006) Modeling aquifer heterogeneity at the facies scale in gravel-sand braided stream deposits. J Hydrol 325:134–153

Zhang C, Li W (2007) Comparing a fixed-path Markov chain geostatistical algorithm with sequential indicator simulation in categorical variable simulation from regular samples. GI Sci Remote Sens 44:251–266

Zinn B, Harvey CF (2003) When good statistical models of aquifer heterogeneity go bad: a comparison of flow, dispersion, and mass transfer in connected and multivariate Gaussian hydraulic conductivity fields. Water Resour Res. doi:10.1029/2001WR001146

 DOI 10.1007/s10040-011-0808-0